Electron kinetics in $He/CH_4/CO_2$ mixtures used for methane conversion

André Janeco, Nuno R. Pinhão and Vasco Guerra

Instituto de Plasmas e Fusão Nuclear, Instituto Superior Técnico, Universidade de Lisboa, 1049-001 Lisboa, Portugal

E-mail: npinhao@ctn.ist.utl.pt

Abstract. In this work the electron kinetics in $He/CH_4/CO_2$ mixtures used for CH_4 conversion is studied, including the contribution of H_2 and CO formed in the discharge, as an initial step to model the reforming of natural gas for *syngas* production in a dielectric barrier discharge. The electron Boltzmann equation for a swarm in the hydrodynamic regime is solved in mixtures of $He/CH_4/CO_2/CO/H_2$ by expanding the electron velocity distribution function (*evdf*) in density gradients and using an iterative method to obtain the angular dependency of the expansion coefficients. The need for such a method in mixtures with CH_4, CO_2 and CO and for the range of E/N values occurring in DBD discharges is assessed. The role of He and the effect of the change in composition by conversion of reagents into products in the *evdf*, transport parameters, reaction rates and power losses is discussed and quantified.

Submitted to: *Plasma Sources Sci. Technol.*

1. Introduction

The search for efficient processes for the conversion of methane to liquid hydrocarbon products, either directly or through the production of *syngas* (a CO/H_2 mixture) intermediate, is an active field of research. Such process would allow the exploration of methane sources from remote areas for the production of methanol or other synthetic liquid fuels with a sufficient energy density to substitute oil-based fuels. Other possible applications include the production of hydrogen for the future hydrogen society. Until now, however, the only viable industrial process is steam reforming, where CH_4 is oxidized by steam in the presence of a catalyst. This process, however, has the disadvantages of operating at high temperature, requiring a slow start and costly materials, and of catalyst deactivation over time.

One of the alternative technologies under investigation is the use of plasma, or the combination of plasma and catalysts, exploiting electron impact collisions and reactions with radicals for gas conversion. Combined with catalysts, plasmas can also supply species and radiation that lower the catalyst activation energy [1, 2].

Since the first studies in the late 1980's [3], a large number of experimental work has been devoted to plasma methane conversion using different types of non-thermal plasmas. Most of the work used dielectric barrier discharges (DBD) frequently associated with a catalyst [4–8]. The most effective types of plasmas and discharge systems tested are gliding discharge systems, alone or associated with a "tornado"-type flow where the gas and electron vibrational temperatures reach values within the (2000-3000) K range [9]. Mixtures of methane with different gases have been studied, the common recipe being methane with an oxidant (oxygen or carbon dioxide are the most common) with a possible addition of a rare gas.

In contrast to the abundant number of experimental work, only a few models of these plasmas have been published. This may be due to the complexity of connecting a description of the filamentary discharges, each occurring in a small volume and on a time frame of tenths of nanoseconds, with the chemical kinetics taking place in the full volume of a reactor and on a much larger time scale. The published models do not consider the process of formation of the filamentary discharges and the associated electron kinetics, analyzing only the chemical kinetics in post-discharge conditions [4, 7, 10, 11]. While in [4] the authors are aware of the dependency of the electron collision rates for the production of methane radicals on the gas composition, electron energy, voltage pulse, etc., they obtain the required parameters from a fit from the experimental results. The other models follow, in different degrees, the same assumptions and approach of [4]. While these models obtained a relative success in reproducing the experimental results and in providing insight on the main processes and reaction paths, their main limitation lies in their specificity to the experimental systems modeled. More recently a self-consistent 1D-model has been published [12] including the discharge formation phase. Although representing a significant step forward in the current understanding of these plasmas, that model describes a homogeneous DBD discharge and does not describe

the characteristic filamentary nature of the discharge in these mixtures. A refinement has since been published, where the filamentary nature of the discharge is simulated through electric field pulses [13]. Another limitation is the use of a two-term Boltzmann solver to obtain the electron transport parameters and rate coefficients, which is known to provide less accurate results in gases with large vibrational excitation cross sections such as CH_4, CO_2 and CO [14, 15]. The development of filamentary discharges also leads to high reduced field values, up to the order of 1000 Td [16], where the two-term approximation becomes insufficient to account for the anisotropy of the electron velocity distribution function (*evdf*). Despite the interest of the modeling results available in the literature, a full self-consistent model of methane plasma conversion is not yet available. The role of electrons on streamer formation and the extreme values of reduced electric field observed during the filamentary discharge determines that such model requires a good description of the electron kinetics on a wide range of fields. We have found, however, only one work [17] discussing, in a very limited way, the electron kinetics in these mixtures. As such we consider important the study of the electron kinetics in these complex mixtures and these fields before reliable global results can be obtained.

Thus, as an initial step for a comprehensive model, we study the electron kinetics in mixtures and conditions relevant for methane conversion in DBD reactors. In the present paper we focus on the $He/CH_4/CO_2$ mixtures used in a previous work [18], where He was experimentally shown to have a relevant role in the conversion. In this paper we show that this effect is a consequence of significant changes in the electron kinetics when He is added to the mixture. We take into account the dissociation of CH_4 and CO_2 in a simplified way, by assuming that the dominant stable products are CO and H_2. Therefore, in practice we study the electron kinetics in a $He/CH_4/CO_2/CO/H_2$ mixture. In the remaining of this paper, we start by discussing the assumptions and representation for the *evdf* used for solving the electron Boltzmann equation. On section 3 we briefly discuss the improvements and modifications made on the cross sections for He, CH_4 and CO_2 in order to make them consistent with the present Boltzmann method, as well as our choice of CO and H_2 cross sections. The results of the electron kinetics are presented in section 4, while the main conclusions are summarized in section 5.

2. Solution of the Boltzmann equation

The behaviour of the electrons is described by the Boltzmann equation for the electron distribution function $f(\vec{r}, \vec{v}, t)$,

$$\frac{\partial f}{\partial t} + \vec{v} \cdot \nabla_r f + \vec{a} \cdot \nabla_v f = C(f) \,, \tag{1}$$

where $\vec{r}$, $\vec{v}$ and t are the position, velocity and time, respectively, $\vec{a} = -(e/m)\,\vec{E}$ denotes the acceleration produced by the external field and $C(f)$ is the linear collision operator accounting for elastic, inelastic and non-conservative collisions. We need to solve (1) taking into account the contribution of new electrons produced in the discharge and

keeping in mind that the relative size of the vibrational cross sections or high reduced field values increases the anisotropy of the *evdf* in velocity space along the field direction.

A good model for the initial phase of the filamentary discharges of DBDs is that of a pulsed Townsend discharge where an electron swarm is emitted in a short time period and drifts in space under a constant electrical field with charge multiplication [19]. While in a filamentary discharge the electric field is not constant, we can admit that the field variations are sufficiently slow and smooth compared to the time and space needed by the *evdf* to equilibrate to these changes. Under the same assumption, we neglect the effect of boundaries on the *evdf*. We further assume that the streamer repetition rate and density is sufficient low to neglect the contribution of the excited molecules and short living radicals on consecutive discharges. This is a good approximation for the purposes of the present investigation. In any case, a full self-consistent model, including the time-dependent chemical kinetics, must take into account the electron kinetics in time-varying fields. Results for the drift velocity of electrons in time resolved rf fields have been calculated in [20] using Monte Carlo simulations.

The analysis of electron swarms developed in [21] can be used if we consider that the electrons are moving in the hydrodynamic regime, meaning that although the electron density grows exponentially, the distribution in velocity space and the transport parameters have reached equilibrium values, independent of their initial values. The theoretical basis of the treatment can be found in [21] and only a short summary of the theory is indicated here to facilitate the discussion.

2.1. Representation of the evdf

The *evdf* is represented as an expansion on space gradients for the electron density [21],

$$f\left(\vec{r},\vec{v},t\right)=\sum_{k=0}^{\infty}F^{[k]}\left(\vec{v}\right)\otimes^{k}\left(-\nabla\right)^{k}\,n\left(\vec{r},t\right) \tag{2}$$

where the expansion coefficients $F^{[k]}\left(\vec{v}\right)$ are velocity-dependent tensors of rank k, $\otimes^k$ is the k-fold inner-product operation and $(-\nabla)^k$ is the k-fold outer product of the gradient operator with itself. The functions $F^{[k]}\left(\vec{v}\right)$ are related to the spatial moments of $f\left(\vec{r},\vec{v},t\right)$ and, in particular, $F^{[0]}\left(\vec{v}\right)=\int f(\vec{r},\vec{v},t)d\vec{r}/\int n(\vec{r},t)d\vec{r}$. Obviously equation (2) reduces to the more common representation for the *evdf* if we neglect the higher order expansion coefficients $F^{[k]},\ k>0$ [see equation (6) below]. A comparison of different representations and methods to solve (1) can be found in [22].

Inserting (2) into equation (1) leads to a hierarchy of kinetic equations for the expansion coefficients $F^{[k]}$:

$$\vec{a}\cdot\nabla_{v}F^{[0]}-C\left(F^{[0]}\right)\ =\ -\,\Omega^{(0)}F^{[0]} \tag{3}$$

$$\vec{a}\cdot\nabla_{v}F^{[k]}-C\left(F^{[k]}\right)\ =\vec{v}F^{[k-1]}-\sum_{j=0}^{k}\Omega^{(j)}F^{[k-j]}\,,\quad k\geq1 \tag{4}$$

where for clarity we have dropped the $\vec{v}$ dependence of $F^{[k]}$. $\Omega^{[j]}$ are generalized transport coefficients and are identified with the ones measured in swarm experiments. These

coefficients are expressed in terms of the functions $F^{[k]}$, the first three corresponding to the transport coefficients

$$\Omega^{(0)} = \Omega = \int (\nu_{\rm ion} - \nu_{\rm att})\, F^{[0]} d\vec{v}$$
$$\Omega^{(1)} = \vec{W} = \int \vec{v} F^{[0]} d\vec{v} + \int (\nu_{\rm ion} - \nu_{\rm att})\, \vec{F}^{[1]} d\vec{v}$$
$$\Omega^{(2)} = \hat{D} = \int \vec{v}\vec{F}^{[1]} d\vec{v} + \int (\nu_{\rm ion} - \nu_{\rm att})\, \hat{F}^{[2]} d\vec{v}$$

where ν are the ionization or attachment frequencies, Ω is the macroscopic effective ionization frequency, $\vec{W}$ is the swarm drift velocity and $\hat{D}$ is the diffusion tensor.

These coefficients may be written [23] as,

$$\Omega^{(k)} = \Gamma^{(k)} + S^{(k)}, \qquad k = 0, 1, 2 \tag{5}$$

(with $\Gamma^{(0)} = 0$) and where $\Gamma^{(k)}$ represents flux and $S^{(k)}$ are source and sink terms resulting from non-conservative interactions. In [24] these terms are called the "flux" and "reactive" components, respectively, while the $\Omega^{(k)}$ are the "bulk" transport coefficients. Without a magnetic field, $\vec{W}$ is parallel to the electric field and $\vec{\Gamma^{(1)}} = \vec{V_d}$. In this case the diffusion tensor, $\hat{D}$ is diagonal with a longitudinal and two equal transversal components. These coefficients are, respectively:

$$D_L = \int v_z F_z^{[1]} d\vec{v} + \int (\nu_{\rm ion} - \nu_{\rm att})\, F_{zz}^{[2]} d\vec{v}$$
$$D_T = \frac{1}{2}\left[\int v_T F_T^{[1]} d\vec{v} + \int (\nu_{\rm ion} - \nu_{\rm att})\, F_{TT}^{[2]} d\vec{v}\right]$$

where the indexes z or T indicate the longitudinal or transverse components. As discussed below we use the set of parameters $\{\Omega^{(0)}, \Omega^{(1)}, \Omega^{(2)}\}$ to adjust the cross sections, while the parameters $\{\Omega^{(0)}, \Gamma^{(1)}, \Gamma^{(2)}\}$, which are used in the solution of the electron fluid equations [15], are discussed in section 4.

2.2. Angular dependence of the distribution function

To solve the set of equations (3, 4) and obtain the expansion coefficients $F^{[k]}(\vec{v})$, $k \leq 2$, we have used a modified version of the algorithm proposed in [25], based on the discrete ordinate S_n method. This algorithm solves the equations on a (v, θ) grid, where $v = |\vec{v}|$ and θ is the angle between $\vec{v}$ and $\vec{E}$, iteratively, using as convergence criteria the relative change on transport parameters. The precision of the angular representation depends on the number of θ intervals used. For radiation transport problems, it has been shown [26] that a discrete ordinate S_{n+1} methods is equivalent to a spherical harmonics P_n expansion. To keep contact with the more commonly adopted representation for the *evdf*, it can be shown that the coefficients, f_n, of the classical multiterm expansion in Legendre polynomials can be obtained from the function $F^{[0]}(\vec{v})$ through the relation

$$f_n(v) = \frac{2n+1}{2} \int F^{[0]}(v, \theta) P_n(\cos\theta) \sin\theta d\theta\,. \tag{6}$$

2.3. Collision term

The collision term includes elastic and 1st and 2nd kind inelastic collisions. The rotational or vibrational populations for each mode, characterized by the gas temperature or a vibrational temperature, T_v, respectively, have been obtained neglecting anharmonic contributions. The superelastic collisions are considered only for vibrations and the cross sections are calculated through the Klein-Rosseland relation. Note that, besides the parent gases, He, CH_4 and CO_2, we take into account the modification of the mixture due to the conversion of CH_4 and CO_2, assuming they are mainly converted into CO and H_2 (*cf.* section 4). Therefore, we solve the Boltzmann equation in the quinary mixture $He/CH_4/CO_2/CO/H_2$.

The non-conservative terms include attachment and ionization. In the latter case we have assumed a 50% energy split between initial and secondary electrons. A realistic projection of the triple differential ionisation cross section has been discussed in [27]. However, as shown in [28], where different possibilities were tested and a comparison between a discrete division of energy among the electrons with a more realistic continuous one was carried out in pure CH_4, the best choice for a discrete energy division is indeed a 50% division. This value is also recommended by [29].

As a rule, electron-electron collisions have not been considered in the present calculations. Nevertheless, a few tests to assess the effect of e-e collisions were carried out. For the two typical values of the reduced electric field considered in this work (*cf.* section 4.1), 74 and 736 Td, the influence of e-e is vanishingly small if the degree of ionisation is lower than 10^{-4} and 10^{-2}, respectively. These results fully justify the neglect of e-e in our calculations, since in DBDs the higher ionisation degrees correspond to the higher electric fields. Accordingly, at the low fields where the *evdf* is sensitive to e-e collisions, the ionization degree is expected to be small, below the values indicated above.

3. Cross Sections

We need to guaranty the consistency between the cross sections used and the representation adopted for the *evdf* to solve (1). In particular, the calculated swarm parameters must adequately reproduce the available experimental data. Most of the cross section sets available in the literature have been adjusted with Boltzmann codes based on the two-term approximation and neglecting or simplifying the contribution of the "reactive" terms in (5). With these codes the measured "bulk" parameters are compared with the computed "flux" parameters. Although the error introduced by this procedure is usually unimportant, in gases with a Ramsauer minimum, like CH_4, or in regions of high field, this introduces an error in the adjusted cross sections [15]. Another advantage of the present method is that, contrarily to most solvers based on the two-term approximation, both the longitudinal and transverse components of $\hat{D}$ are computed and compared with the experimental values.

Complete and consistent sets of cross-sections for He, CH_4 and CO_2 were developed. They are based on a revision and adjustment of published cross-section sets and ensure a good agreement between the measured transport parameters and those calculated with the current method. For the present paper we have revised and adjusted various cross sections reported by different authors for the gases under study in order to obtain cross section sets consistent with the representation of the *evdf*, and only a brief summary is presented here. We focused in obtaining a good agreement on the effective ionization coefficient as it indicates that we are obtaining well estimated reactive components of the bulk transport coefficients terms in eq.5. In the modifications introduced we have tried to keep the original total inelastic cross section. Due to the lack of experimental data for the transport parameters in gas mixtures, the validation of the cross sections was done for each gas individually, comparing the calculations and measurements of the swarm parameters in pure gases.

In what concerns CH_4, we have started with the cross section set from Pinhão [30]. The latter is based on the set from Shirai [31], complemented with the vibrational excitation from M. C. Bordage [28] and the electron attachment from Rawat [32]. For $E/N > 300$ Td we compare our α/N calculations with the experimental measurements of Davies [33], as reported in the IST-Lisbon and LAPLACE databases [34, 35], while for $E/N < 300$ Td we consider the measurements from Urquijo [36]. We also aimed at adjusting the relation between the ionization and attachment coefficients, approaching the values reported by Hunter [37] above 150 Td. To achieve a good calculation of the effective ionization coefficient, α/N, we have reduced the cross section for attachment and raised the dissociative excitation to CH_2 (scaled respectively to 0.1 and 1.4), as compared with [30]. The change in the attachment cross section makes it closer to those suggested by Davies [33] in IST-Lisbon database [34]. The change in the cross section for excitation to CH_2 does not significantly change the total inelastic cross section or the total dissociation as the cross section for CH_3 is dominant. With these modifications a significant improvement is obtained on the calculated values of α/N. The original set lead to large relative differences between the calculated and measured α/N values below 150 Td. With the modifications the range of accurate values of α/N goes as low as ~ 90 Td. Considering an uncertainty of 5% in the experimental measurements, the reduced χ^2 improves from 4.2 to 1.8 when comparing the experimental values with, respectively, the calculations with the original set above 150 Td and with the modified set above 85 Td. Figure 1 a) shows the comparison between the calculated and the experimental effective ionization coefficient.

The He cross section set was adjusted from Belmonte [41]. In order to obtain a good agreement between the calculated value of the effective ionization coefficient and the experimental data from Chanin [38], Davies [39], Lakshminarasimha [40] (taken from the IST-Lisbon database [34]) at the breakdown fields, we had to slightly increase the ionization cross section, scaled to 1.2. To compensate for the change on the total inelastic cross section we decreased two electronic cross sections (2^3S and 2^1P), scaled to 0.4 and 0.7 respectively. Figure 1 b) shows the comparison between the calculated

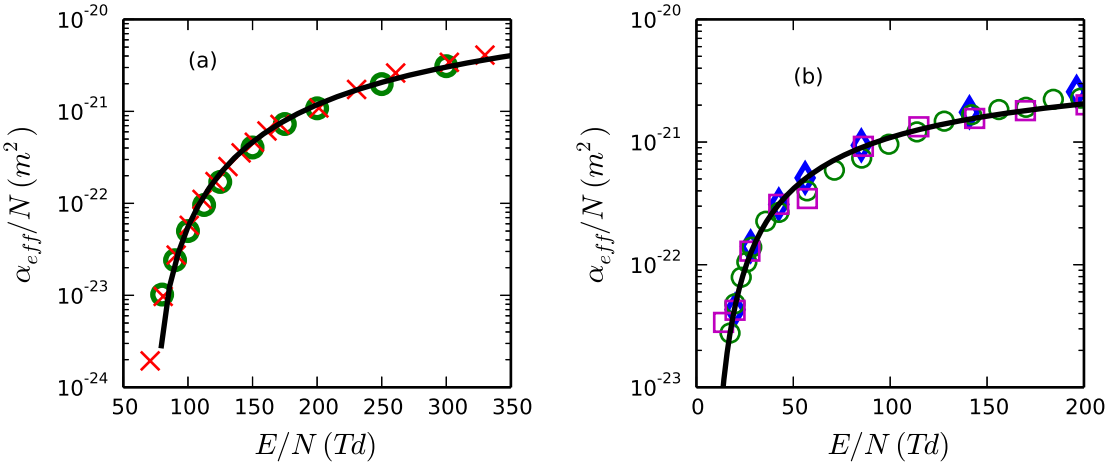

Figure 1. Calculated (—) and experimental (○ [33], × [36] for *a*; ◇ [38], ○ [39], □ [40] for *b*) effective ionization coefficient in CH_4 (a) and He (b).

and the experimental effective ionization coefficient.

Regarding CO_2, our base was the cross section set by Nakamura [42], available at the NIFS database [43]. We have modified the momentum transfer cross section and the lower energy region of the first vibrational cross section (010 bending mode), making them closer to those of Hayashi [44]. Buckman and co-workers [45] report an increase of the electron scattering cross section with the vibrational population (mainly of the bending mode). However, as discussed in section 4, we have only considered conditions of low vibrational excitation and have thus neglected this effect. The resulting new cross sections are shown in figure 2. These adjustments were dictated by the comparison of the calculated mobility and diffusion coefficients with the experimental values from Elford [46], as reported in [35]. As an example, figure 3 shows the calculated and experimental electron mobility for reduced fields below 20 Td. Before the adjustment the discrepancy with the experimental values was larger than 10%. Additionally, we have included dissociative excitations and ionizations cross sections, as reported in Itikawa [47], ignoring those with thresholds above 80 eV. The addition of these cross sections was made ensuring we have kept the same total inelastic cross-section.

Finally, the cross sections for CO and H_2 were taken from Buckman and Phelps [48], with CO being based on Land [49]. CO cross sections were retrieved with no modifications while for H_2 we used the scale factors suggested in the Phelps database [50] for the rotational transitions (for J = 0 → 2 divide by 0.25; for J = 1 → 3 divide by 0.75).

4. Results and discussion

A full study of the effect of composition on the electron kinetics requires the knowledge of the cross sections for the different species resulting from CH_4 and CO_2 dissociation and

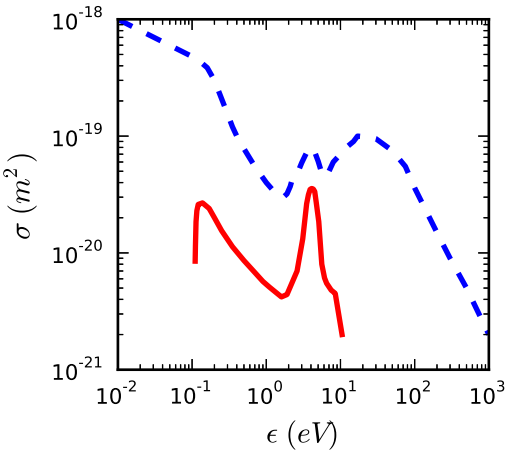

Figure 2. Modified cross sections of CO_2 used in this work. (– – –) Elastic momentum transfer; (——) 010 vibration.

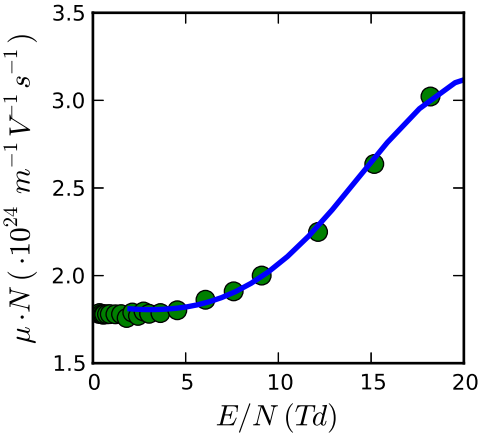

Figure 3. Calculated (——) and experimental (•) [46] electron mobility coefficient in CO_2.

the coupling with the chemical kinetics. In most cases, however, the concentrations of the dissociation products are relatively low and their cross sections are not well known. Here, we have adopted a simplified model, where H_2 and CO are assumed to be the dominant stable products from this dissociation, such that the formula

$$CH_4 + CO_2 \rightarrow 2H_2 + 2CO \tag{7}$$

is valid. Accordingly, we study $He/CH_4/CO_2/H_2/CO$ mixtures, as the result from a conversion process of an initial $He/CH_4/CO_2$ mixture. Following (7), we consider a constant $[CH_4]/[CO_2]$ concentration ratio of one. The concentrations are determined by only two parameters, (η, C): η is the He fractional concentration on the base $He/CH_4/CO_2$ mixture, and was ranged from 0 to 1; C is the conversion ratio of both

Gas	He	CH_4, CO_2	H_2, CO
Concentration	η/α	$(1-C)(1-\eta)/(2\alpha)$	$C(1-\eta)/\alpha$

Table 1. Concentration of each gas in the mixture as a function of (η, C), the He concentration and value of conversion for CH_4 or CO_2, respectively. $\alpha = 1 + C(1-\eta)$.

(η, C)	He	CH_4, CO_2	H_2, CO
$(0, 0)$	0	0.5	0
$(0.6, 0)$	0.6	0.2	0
$(0, 0.3)$	0	0.27	0.23
$(0.6, 0.3)$	0.54	0.12	0.11

Table 2. Concentration of each gas in the mixture as a function of (η, C), the He concentration and value of conversion for CH_4 or CO_2, respectively.

CH_4 and CO_2,

$$C = \frac{[X]_0 - \alpha[X]}{[X]_0} \tag{8}$$

where $[X]$ is the fractional concentration of the species X, the index 0 refers to the initial mixture, and α is the expansion factor, N/N_0, resulting from the increase in the number of molecules with the conversion, and corresponds to α in equations (3) and (4) in [18]. The relative increase of the number of molecules, α, can be written in terms of (η, C),

$$\alpha = 1 + C(1-\eta) \tag{9}$$

so that the mixture composition depends only on these two parameters. The concentration of each gas in the mixture can be retrieved from the expressions indicated in table 1. The (η, C) values most often used in this article are $(0, 0)$, $(0.6, 0)$, $(0, 0.3)$ and $(0.6, 0.3)$, see table 2. The former two represent mixtures without or with a significant He concentration before conversion, respectively, while the latter two represent the same initial mixtures after a conversion of 30%. These (η, C) values were chosen as representative of typical compositions and capable of showing the effects of dissociation on the electron kinetics. They were based on experimental results [18]. In an actual discharge, the real mixture is more complex and constantly changing. Along with other molecules with lower concentrations, many radicals with relevant electron collision cross sections will be present. These gases can significantly influence the chemical kinetics and cannot be neglected from a chemical model. For example, the different ionization thresholds change the effective ionization coefficient of the mixture. Although this model does not consider all the species formed in a DBD discharge, it should provide qualitative information on the effect of composition in the electron kinetics.

All the results were computed at room temperature ($T_g = 300$ K). The population of vibrational excited levels of the molecular gases (CH_4, CO_2, H_2 and CO) are assumed

to follow a Boltzmann distribution for each mode at $T_V = T_g$. Accordingly, only levels with $v = 0$ or $v = 0, 1$ (depending on the energy separation of the series) and a pseudo-level corresponding to the sum of the remaining populations, have been considered. In the case of hydrogen, we also took into account the rotational population of the two spin isomers. The effect of these vibrational or rotational excited levels is negligible for most of the gases and conditions considered, except for CO_2 in a limited range of E/N, where it is responsible for a 1% change on the drift velocity and up to 7% change on the longitudinal diffusion coefficient, D_L. Note, however, that usually $T_V \neq T_g$ and vibrational excited levels can significantly influence the electron kinetics [51]. The study of this effect will be the subject of a future publication.

The results were obtained with an angular grid with 31 equally spaced points, a velocity grid with a step of 6×10^3 m/s and an adjustable number of points, such that the difference between the integral of the expansion coefficient $F^{[0]}$ and one is always less than 10^{-8}. Finally the convergence criteria for the transport parameters was to obtain a relative difference $\leq 10^{-6}$ between successive iterations, as it has given us results comparable with other proven techniques [22].

4.1. Isotropic coefficient, f_0

To facilitate the comparison of our calculations with results based on the two-term approximation we show in figure 4 the isotropic component, f_0, obtained from (6), for three values of reduced field and different combinations of (η, C). 736 Td represents a high field, as found in streamer formation space charge fields [52], 74 Td represents a DBD disruption field [53], and 10 Td is a low field at which electrons do not have enough energy for most inelastic processes interesting for dissociation. As it can be seen, the presence of He is responsible for a shift of the isotropic component to higher energies, with an increase of the number of high energy electrons and a reduction of the number of electrons with low energy. This effect is clearly visible both at low and high E/N values but the electron energy at which the f_0 curves for different He concentrations cross is greater for higher E/N values. It is a direct consequence of the shape and amplitude of the electron impact cross sections, which are globally smaller in He than in the molecular gases, and have a smaller threshold for the inelastic processes in the later gases.

Figure 4 further shows that the effect of conversion is qualitatively different than the He addition. In any case, for intermediate and low values of E/N, the detailed shape of f_0 is significantly modified in the low-energy region. This modification induces marked changes in the electron transport parameters, as detailed below. Increasing the H_2 and CO concentrations the decrease of f_0 with energy is more pronounced, mainly because of the important CO vibrational excitation cross sections that have the maximum below 2 eV. Note that the mixtures with H_2 and CO have a higher fraction of molecular gases. On the other hand, for higher energies, where electronic excitations and ionizations take place, H_2 and CO have a smaller total inelastic cross section than the CH_4 and CO_2

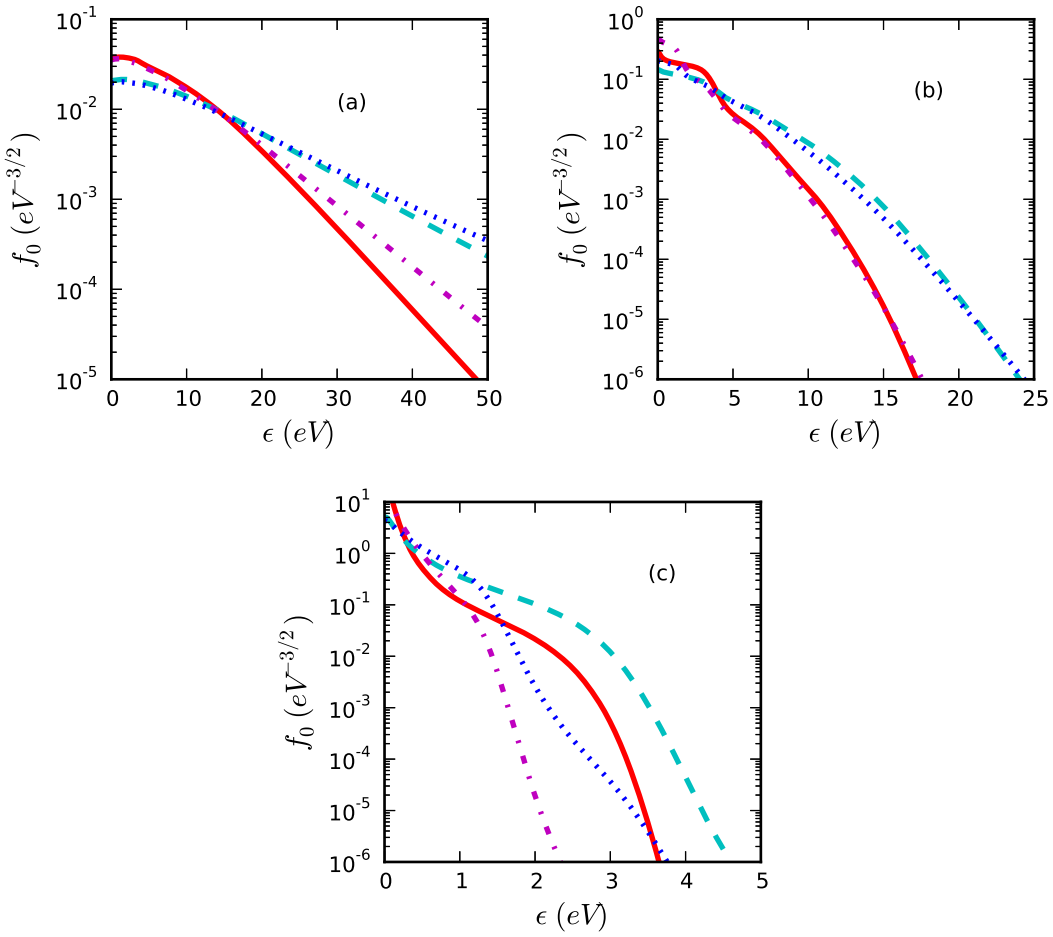

Figure 4. Isotropic component of the electron energy distribution function as a function of the electron energy for three values of reduced field, 736 Td (a), 74 Td (b) and 10 Td (c), and different combinations of (η, C), where η is the initial He concentration and C the conversion level: (——) $(0, 0)$; (– – –) $(0.6, 0)$; (— · —) $(0, 0.3)$; (· · · · · ·) $(0.6, 0.3)$.

they substitute. This justifies the crossing seen in f_0 for $E/N = 736$ and 74 Td (figure 4a and 4b), between 15 and 25 eV, where the mixtures with H_2 and CO have a larger population of electrons at high energies.

4.2. Transport parameters

As previously referred, experimental transport parameters in these mixtures are not available. As such, we present these transport parameters calculated for a wide range of fields. These results can be used as input data in the drift diffusion equation for electrons. The flux drift velocity is represented as a function of E/N in figure 5, for the same values of (η, C) considered before. As the figure illustrates, the mixture of the two gases results in a flux drift velocity with a pronounced hump between (2–100) Td. It is worth noting the marked influence of the conversion of CH_4 and CO_2 in this region,

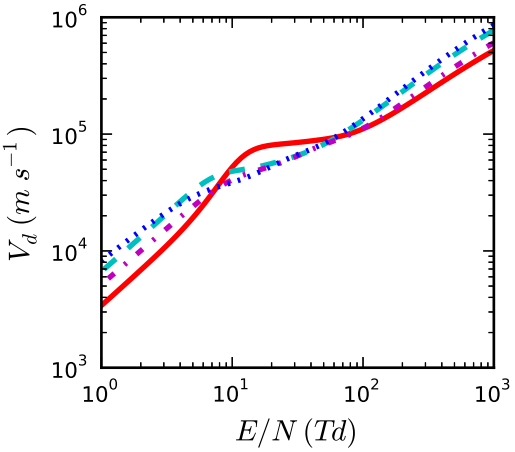

Figure 5. Flux drift velocity as a function of the reduced field and for different combinations of (η, C): (——) $(0,0)$; (– – –) $(0.6,0)$; (— · —) $(0,0.3)$; (· · · · · ·) $(0.6,0.3)$.

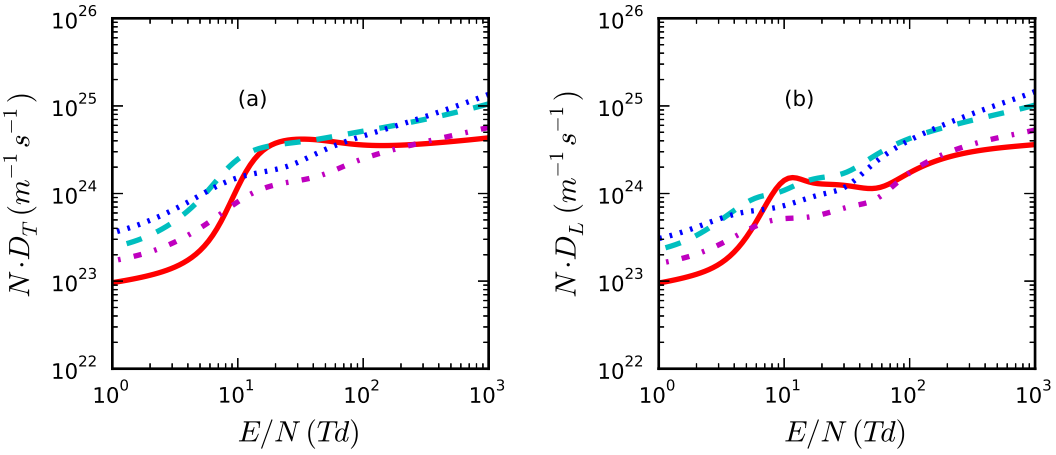

Figure 6. Transverse (a) and longitudinal (b) components of the diffusion tensor as a function of the reduced field and for different values of (η, C): (——) $(0,0)$; (– – –) $(0.6,0)$; (— · —) $(0,0.3)$; (· · · · · ·) $(0.6,0.3)$.

as a consequence of the modifications in the *evdf* at low energies. The admixture of He or an increase in conversion has the effect of smoothing down and eventually eliminate this hump.

Figure 6 shows the longitudinal and transverse components of the diffusion tensor for different values of (η, C). The CH_4/CO_2 mixture also shows a hump in the same range as the flux drift velocity. An increase in C leads to the disappearance of the hump (or even to a depression in the case of D_L) and to an increase of the values of diffusion bellow ~ 10 Td. The admixture of He increases the diffusion in almost the full range of values studied.

Figure 7 shows that the effective ionization coefficient around the breakdown field

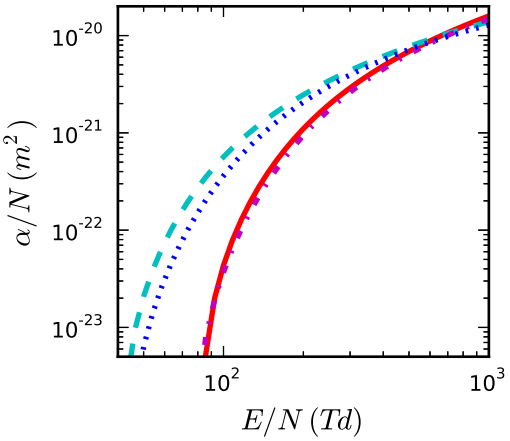

Figure 7. Effective ionization coefficient as a function of the reduced field and for different values of (η, C): (——) $(0,0)$; (– – –) $(0.6,0)$; (— · —) $(0,0.3)$; (· · · · · ·) $(0.6,0.3)$.

(below 100 Td for a typical DBD) is highly dependent on the He concentration. For these field values, although the He addition corresponds to a decrease of the relative concentrations of CH_4 and CO_2, which have lower ionization thresholds than He and, therefore, are easier to ionize (*cf.* as well figure 8), the increase in the high energy tail of f_0 discussed in figure 4 determines a significant increase in the ionization efficiency. The increase of α/N with He explains the reduction in breakdown voltage observed in these mixtures [18]. If we account for the conversion of reagents into H_2 and CO, we obtain a decrease in the effective ionization coefficient. This is due to the slightly higher ionization thresholds for H_2 and CO (15 and 14 eV respectively) as well as to the reduction of He concentration with conversion.

4.3. Collision frequencies

The increase in the tail of the isotropic component, f_0, with He is responsible for a large increase in the electronic excitation or ionization rate coefficients of CH_4 and CO_2. Higher rates, however, do not automatically translate into more excitation or ionization processes since the reagents concentrations are reduced with the inclusion of He. To evaluate the net effect of He we need to take into account as well the changes in the relative concentrations of CH_4 and CO_2 with He. In order to do that we analyze the reduced collision frequencies, defined as

$$\nu_M/N = [M]C_e^X \ , \tag{10}$$

where N is the total gas density, [M] is the fractional concentration of species M, with $M = CH_4$ or CO_2, and C_e^X is the electron impact rate coefficient for process X. In this way we will be analysing the already combined effect of the change in the rate coefficients (because of the modifications of the *evdf*) and the change of the species densities.

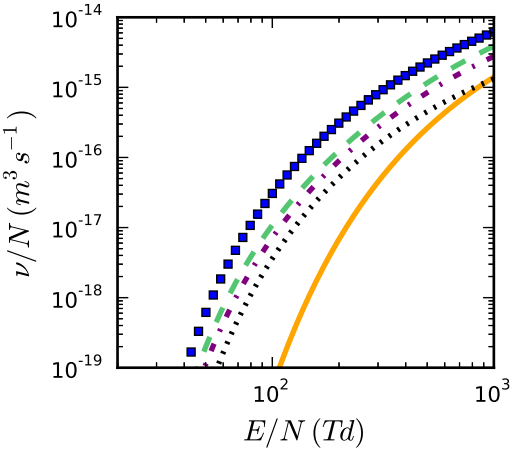

Figure 8. Ionization reduced frequencies for He (——), CH_4 (■), CO_2 (– – –), CO (— · —) and H_2 (· · · · · ·) as a function of the reduced field for a (η, C) value of $(0.6, 0.3)$.

Figure 8 shows the ionization reduced collision frequencies of He, CH_4, CO_2, H_2 and CO for a (η, C) value of $(0.6, 0.3)$. It confirms that the dominant He influence on α/N is due to the increase of f_0, rather than to a modification of the ionization channels. In fact, the major contributor to the ionizations remains CH_4.

Figure 9 shows the variation of the reduced collision frequencies for formation of CH_3 through dissociative excitation of CH_4 and dissociation of CO_2 through the formation of $O(^1S)$, for different combinations of (η, C). In both cases and in the range studied, the collision frequencies increase with He and this increase is more significant at low E/N values. The introduction of He in the system has two competing effects: it increases the tail of f_0 and at the same time decreases the reagents' concentration. The net effect depends on the amount of He and on the reduced electric field. Considering figure 9, it is observed that the dissociation frequencies for a 60% He addition are lower than without He only at the highest field values shown. For lower field values, the maximum in the dissociation frequencies occurs at even higher He concentrations. For example, at 250 Td the maximum of dissociation collision frequency is obtained at 80% He, while at 75 Td it occurs at 90% He. The collision frequencies decrease with C and this decrease is stronger than the mere decrease in the corresponding concentrations, since f_0 becomes slightly depleted in the relevant region of energies, right above the thresholds of 7.5 and 12 eV, respectively for CH_4 and CO_2 (*cf.* figure 4).

Regarding helium, decreasing its concentration significantly reduces the He collision frequencies. In this case, both the reduction in concentration and the modification in the tail of f_0 contribute to this effect, acting on the same direction. This is in contrast with what happens with the molecular gases, where the two effects compete. Figure 10-a) compares the collision frequencies for production of He^+ as a function of E/N for three values of η. Figure 10-b) compares the collision frequencies for the excitation of the two metastable states of He ($2\,^3S$ and $2\,^1S$) for the same conditions. Thus, a greater

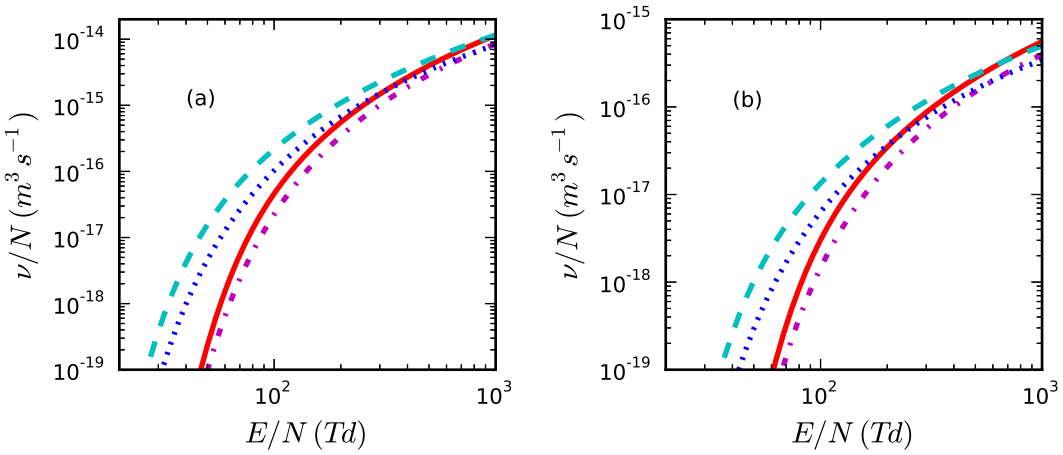

Figure 9. Dissociative electronic excitation reduced frequencies for $CH_4 \rightarrow CH_3$ (a) and $CO_2 \rightarrow O(^1S)$ (b) as a function of the reduced field and for different values of (η, C): (——) $(0, 0)$; (– – –) $(0.6, 0)$; (— · —) $(0, 0.3)$; (· · · · · ·) $(0.6, 0.3)$.

production of He excited species and ions is obtained with higher He concentration. It is also interesting to compare the collision frequencies of He metastables excitation from figure 10-b) with those of CH_4 or CO_2 dissociative electronic excitation or ionization from figures 9 and 8. For $[He] = 0.6$ the He metastables production is much slower than the direct electronic excitation or ionization of CH_4 or CO_2. As can be verified from figures 8 and 10b, the CH_4 ionization collision frequency is always more than one order of magnitude higher than the metastables excitation of He. Note that in figure 8 a value $C = 0.3$ was considered, so that an exact comparison would involve even higher values of the CH_4 ionization reduced collision frequency. From these results we expect that Penning ionization of CH_4 or CO_2, through collision with He metastables, cannot compete with direct electronic collision ionization. A definite conclusion, however, needs chemical kinetics calculations.

The analysis of the low-energy threshold processes, in particular vibrational excitation, is more complex. Figure 11 shows the total reduced vibrational excitation frequencies for CH_4 and CO_2 as a function of E/N and for different (η, C) values. Contrary to the processes with higher thresholds, the vibrational collision frequencies do not increase with He for the full E/N range studied. The discussion in section 4.1 contributes to a better understanding of this behavior. The main influence of He in f_0 is to increase the tail, at the cost of reducing the fraction of electrons with lower energies. Therefore, f_0 curves for different He concentrations cross at a given energy u_c. Without He f_0 is higher for electron energies below u_c, while with He f_0 is higher for electron energies above u_c. The value of u_c depends on the reduced field, increasing with E/N. Figure 4 clearly shows that only for E/N values lower than ~ 10 Td can He have a positive effect on f_0 in the energy range relevant for vibrational excitations, since at this E/N value the curves cross at energies close to the vibrational excitation threshold. As shown below, the vibrational collisions are extremely important power

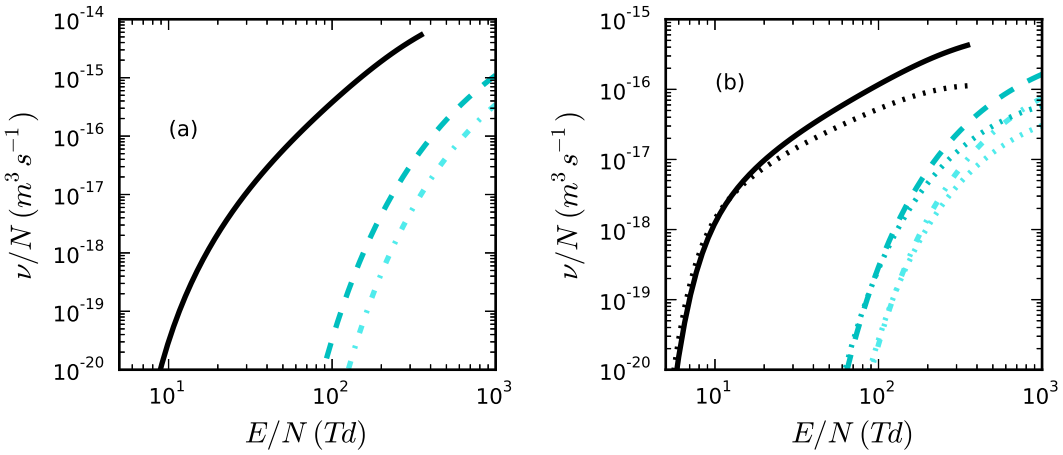

Figure 10. Electron collision reduced frequencies for He ionization (a) and excitation of He metastables (b) as a function of the reduced field and for different values of (η, C). For ionization and $2\,^1S$, (——) $(1,0)$; (– – –) $(0.6,0)$; (— · —) $(0.4,0)$. For $2\,^3S$: the dotted curves (· · · · · ·) with the same colors as before.

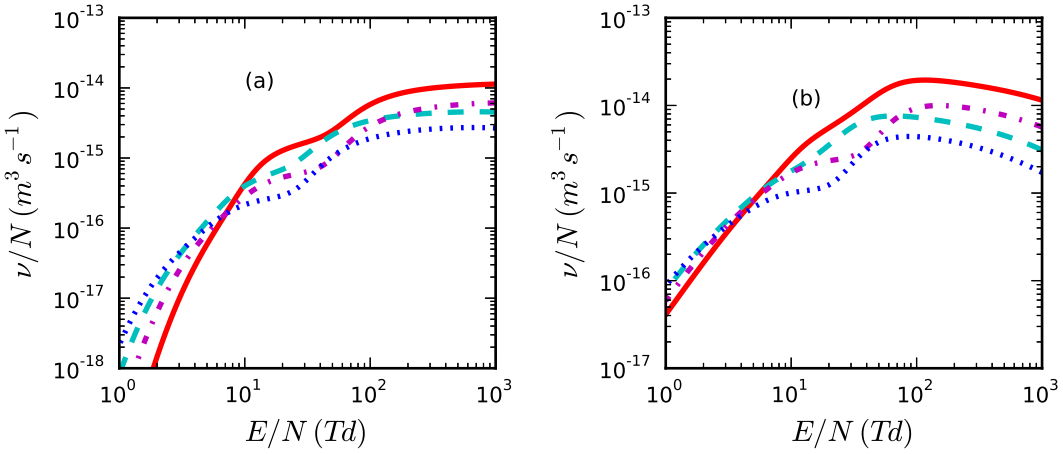

Figure 11. Total vibrational reduced collision frequencies in CH_4 (a) and CO_2 (b) as a function of the reduced field and for different values of (η, C): (——) $(0,0)$; (– – –) $(0.6,0)$; (— · —) $(0,0.3)$; (· · · · · ·) $(0.6,0.3)$.

losses and, for the reduced field ranges relevant for dissociation, the He dilution has the positive effect of decreasing these losses and redirecting them to dissociative processes. A similar effect is observed from the inclusion of H_2 and CO.

4.4. Absorbed Power

A possible misconception about He dilution is that the decrease in the reagents' concentrations would determine a worse conversion efficiency. Although the dilution on most other molecular gases indeed determines a worse conversion efficiency [54], with a lower power channeled to dissociation, this is not the case with He, as anticipated by

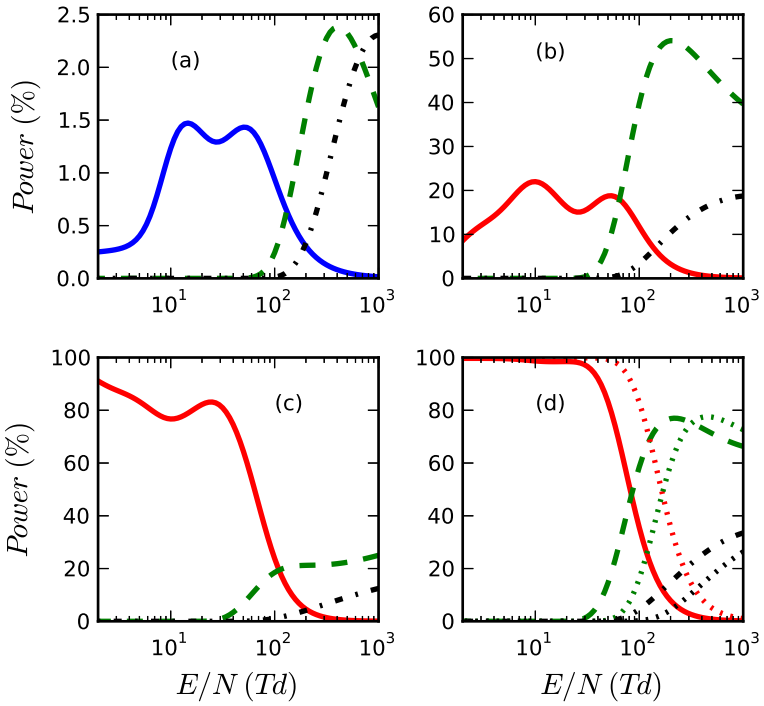

Figure 12. Fractional power losses for each type of process on each of the mixtures' components, He (a), CH_4 (b), CO_2 (c), and on the whole mixture (d), as a function of the reduced field: (——) momentum transfer; (——) vibrational excitation; (– – –) electronic excitation; (— · —) ionization. All the calculations are made for $(\eta, C) = (0.6, 0)$, with the exception of the dotted curves (· · · · · ·) in (d), corresponding to $(\eta, C) = (0, 0)$.

inspection of figure 9. To further clarify this issue and quantify the effect, we now look at the fractional power losses in the various collision processes, including the dissociation of CH_4 and CO_2.

Figure 12 shows the fractional power losses in the different electron-collision processes occurring in each gas for a given mixture. At a value of η of 0.6, the fraction of power going to any type of process in He is always below 2.5%, and the sum of all power losses in He is always below 5%, with the elastic losses dominating for $E/N \leq 100$ Td. This is a consequence of the much more important cross sections of the molecular gases and also of the very high threshold for inelastic processes in He. For fields up to 60 Td, the power is absorbed almost entirely on the vibrational excitation of CH_4 and CO_2. Only around 40 Td does the electronic excitations become significative. Above $\sim$ 100 Td, electronic excitations become the dominant power sinks, with a maximum share of power consumption of about 80% at 200 Td. The ionization channels only have an impact on deletedthe power consumption above 100 Td. They have a growing trend with the reduced field, reaching approximately 35% at our maximum of 1000 Td.

In CH_4 most inelastic processes are dissociative, with the most important process being the dissociative excitation into CH_3. We consider dissociative excitation into

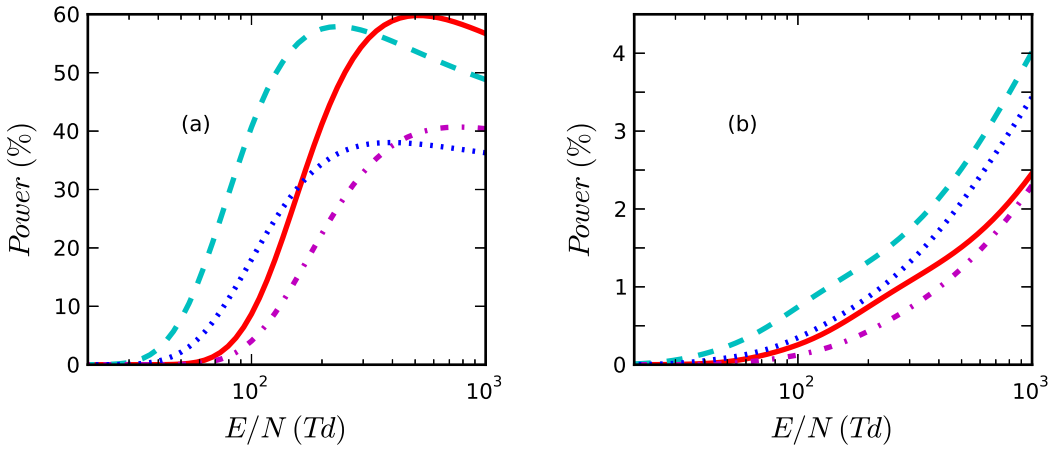

Figure 13. Fractional power losses on dissociative processes of CH_4 (a) and CO_2 (b) as a function of the reduced field and for different values of (η, C): (——) $(0, 0)$; (– – –) $(0.6, 0)$; (— · —) $(0, 0.3)$; (· · · · · ·) $(0.6, 0.3)$.

CH_3, CH_2 and CH, dissociative ionization into CH_3^+, CH_2^+, CH^+, C^+, H_2^+ and H^+, and dissociative attachment into CH_2^- and H^-. As for CO_2, we consider dissociative excitation forming O^1S, dissociative attachment producing O^-, and the dissociative ionization into C^+, O^+ and CO^+. Figure 13 shows the fractional power losses in the dissociative processes of CH_4 and CO_2. Figure 13a reveals that the addition of He does not significantly change the total energy directed to the dissociation. Instead, its main effect is to shift the maximum of dissociation to lower reduced field values. The same conclusion can be inferred from figure 12b. This means that higher fields do not necessarily imply a higher conversion efficiency of CH_4. On the other hand, CO_2 has a continuously growing trend for the fraction of power going into dissociative processes with the increase of the reduced field, as depicted in figure 13b. With its low power absorption, the addition of He is very important for CO_2 dissociation, as it can double the fraction of power absorbed by this channel.

5. Conclusions

The analysis of the electron kinetics in CH_4/CO_2 plasmas used for *Syngas* production is essential to understand the complex chemistry that takes place in these discharges. The addition of other gases, such as He or the species resulting from the electron collisions, can significantly change the *evdf*, the electron reaction rates and the energy losses. We have thus investigated the electron kinetics in the quinary mixture $He/CH_4/CO_2/CO/H_2$ under simplifying assumptions.

The role of He in $He/CH_4/CO_2$ discharges has been evaluated. Except for very high values of He concentration, the excitation and ionization frequencies in He are very low. The dominant electron energy loss processes in He for E/N values up to 100 Td are elastic collisions. However, the collisions in He allow a significant shift of the *evdf*

to higher energy and are responsible for an increase of the electronic excitation and ionization frequencies in CH_4 and CO_2. The He is also responsible for a shift of the effective ionization curve to lower E/N values. Note, however, that the ionization takes place in collisions with CH_4, CO_2 and their products and not with He. The current results do not support the suggestion that Penning ionization resulting from collisions with He metastable atoms may have a significant contribution to the discharge [55], since the frequency for excitation of these levels is very low. It is expected that the same qualitative behavior should be obtained replacing He by other atomic gases.

The effect of the change in composition with conversion on the electron kinetics depends on E/N and on the specific process analyzed. In the one hand, the processes with a low energy threshold, such as vibrational excitation, show an increase in the collision frequencies with CH_4 and CO_2 conversion bellow a given value of E/N; however, as E/N increases, the collision frequency becomes negatively affected by this change in composition. On the other hand, collision processes with higher thresholds are much less sensitive to the degree of conversion and the collision frequencies for those processes are approximately proportional to concentration.

The importance of vibrations of CH_4, CO_2, but also of CO and H_2 should direct future work to the role of vibrational excited states on the electron kinetics and on the chemistry of dissociation. As a matter of fact, warm plasmas provide interesting conditions and results, that still require a deeper understanding of the underlaying electron kinetics [9, 56, 57].

Acknowledgments

We acknowledge financial support from Portuguese FCT through the PhD grant SFRH/BD/63234/2009, project PTDC/FIS-PLA/2135/2012 and Pest-OE/SADG/LA 0010/2011.

References

[1] H.-H. Kim, "Nonthermal Plasma Processing for Air-Pollution Control: A Historical Review, Current Issues, and Future Prospects," *Plasma Processes and Polymers*, vol. 1, no. 2, pp. 91–110, 2004.

[2] N. A. S. A. Istadi, "Co-generation of synthesis gas and C_2^+ hydrocarbons from methane and carbon dioxide in a hybrid catalytic-plasma reactor: A review," *Fuel*, vol. 85, pp. 577–592, Mar. 2006.

[3] R. G. Mallinson, C. M. Sliepcevich, and S. Ruse, "Methane Partial Oxidation in Alternating Electric Fields," in *Proc. Amer. Chem. Society*, vol. 32, (San Francisco), American Chemical Society, 1987.

[4] M. Kraus, W. Egli, K. Haffner, B. Eliasson, U. Kogelschatz, and A. Wokaun, "Investigation of mechanistic aspects of the catalytic CO_2 reforming of methane in a dielectric-barrier discharge using optical emission spectroscopy and kinetic modeling," *Physical Chemistry Chemical Physics*, vol. 4, pp. 668–675, Feb. 2002.

[5] S.-S. Kim, B. Kwon, and J. Kim, "Plasma catalytic methane conversion over sol–gel derived Ru/TiO2 catalyst in a dielectric-barrier discharge reactor," *Catalysis Communications*, vol. 8, pp. 2204–2207, Dec. 2007.

[6] A. Indarto, "A review of direct methane conversion to methanol by dielectric barrier discharge," *IEEE Transactions on Dielectrics and Electrical Insulation*, vol. 15, no. 4, pp. 1038–1043, 2008.

[7] A. Indarto, N. Coowanitwong, J.-W. Choi, H. Lee, and H. K. Song, "Kinetic modeling of plasma methane conversion in a dielectric barrier discharge," *Fuel Processing Technology*, vol. 89, pp. 214–219, Feb. 2008.

[8] X. Tu, H. J. Gallon, M. V. Twigg, P. a. Gorry, and J. C. Whitehead, "Dry reforming of methane over a Ni/Al_2O_3 catalyst in a coaxial dielectric barrier discharge reactor," *Journal of Physics D: Applied Physics*, vol. 44, p. 274007, July 2011.

[9] A. Gutsol, A. Rabinovich, and A. Fridman, "Combustion-assisted plasma in fuel conversion," *Journal of Physics D: Applied Physics*, vol. 44, p. 274001, July 2011.

[10] S. A. Nair, T. Nozaki, and K. Okazaki, "Methane oxidative conversion pathways in a dielectric barrier discharge reactor–Investigation of gas phase mechanism," *Chemical Engineering Journal*, vol. 132, no. 1-3, pp. 85–95, 2007.

[11] J. Luche, O. Aubry, A. Khacef, and J.-M. Cormier, "Syngas production from methane oxidation using a non-thermal plasma: Experiments and kinetic modeling," *Chemical Engineering Journal*, vol. 149, pp. 35–41, July 2009.

[12] C. De Bie, B. Verheyde, T. Martens, J. van Dijk, S. Paulussen, and A. Bogaerts, "Fluid Modeling of the Conversion of Methane into Higher Hydrocarbons in an Atmospheric Pressure Dielectric Barrier Discharge," *Plasma Processes and Polymers*, vol. 8, pp. 1033–1058, Nov. 2011.

[13] R. Snoeckx, R. Aerts, X. Tu, and A. Bogaerts, "Plasma-Based Dry Reforming: A Computational Study Ranging From Nanoseconds to Seconds Timescale," *The Journal of Physical Chemistry A*, vol. 4, Feb. 2013.

[14] L. C. Pitchford and A. V. Phelps, "Comparative Calculations of Electron-swarm Properties in N_2 at Moderate E/N Values," *Physical Review A*, vol. 25, pp. 540–554, 1982.

[15] Z. Lj. Petrović, S. Dujko, D. Marić, G. Malović, v. Nikitović, O. Šašić, J. Jovanović, V. Stojanović, and M. Radmilović-Rađenović, "Measurement and interpretation of swarm parameters and their application in plasma modelling," *Journal of Physics D: Applied Physics*, vol. 42, p. 194002, Oct. 2009.

[16] G. V. Naidis, "Modelling of transient plasma discharges in atmospheric-pressure methane–air mixtures," *Journal of Physics D: Applied Physics*, vol. 40, pp. 4525–4531, Aug. 2007.

[17] D. W. Larkin, L. L. Lobban, and R. G. Mallinson, "The direct partial oxidation of methane to organic oxygenates using a dielectric barrier discharge reactor as a catalytic reactor analog," *Catalysis Today*, vol. 71, no. 1-2, pp. 199–201, 2001.

[18] N. R. Pinhão, A. Janeco, and J. B. Branco, "Influence of Helium on the Conversion of Methane and Carbon dioxide in a Dielectric Barrier Discharge," *Plasma Chemistry and Plasma Processing*, vol. 31, pp. 427–439, Mar. 2011.

[19] V. I. Gibalov and G. J. Pietsch, "The development of dielectric barrier discharges in gas gaps and on surfaces," *Journal of Physics D: Applied Physics*, vol. 33, no. 20, p. 2618, 2000.

[20] S. Bzenić, Z. Lj. Petrović, Z. M. Raspopović, and T. Makabe, "Drift velocities of electrons in time varying electric fields," *Jpn. J. Appl. Phys.*, vol. 38, p. 6077, 1999.

[21] K. Kumar, H. R. Skullerud, and R. E. Robson, "Kinetic Theory of Charged Particle Swarms in Neutral Gases," *Australian Journal of Physics*, vol. 33, pp. 343–448, 1980.

[22] N. R. Pinhão, Z. Donkó, D. Loffhagen, M. J. Pinheiro, and E. a Richley, "Comparison of kinetic calculation techniques for the analysis of electron swarm transport at low to moderate E/N values," *Plasma Sources Science and Technology*, vol. 13, no. 4, pp. 719–728, 2004.

[23] R. E. Robson, "Transport Phenomena in the Presence of Reactions: Definition and Measurement of Transport Coefficients," *Australian Journal of Physics*, vol. 44, no. 6, pp. 685–692, 1991.

[24] A. M. Nolan, M. J. Brennan, K. F. Ness, and A. B. Wedding, "A benchmark model for analysis of electron transport in non-conservative gases," *Journal of Physics D: Applied Physics*, vol. 30, pp. 2865–2871, 1997.

[25] P. Segur, M. Yousfi, and M. C. Bordage, "Comparisons between different methods of solution of

the Boltzmann equation adapted to the calculation of swarm parameters in a weakly ionised medium," *Journal of Physics D: Applied Physics*, vol. 17, pp. 2199–2214, 1984.

[26] D. E. Cullen, "Why are the Pn and Sn methods equivalent," tech. rep., Lawrence Livermore National Laboratory, 2001.

[27] C. Opal, W. Peterson, and E. Beaty, "Measurements of Secondary-Electron Spectra Produced by Electron Impact Ionization of a Number of Simple Gases," *The Journal of Chemical Physics*, vol. 55, pp. 4100–4106, Oct. 1971.

[28] M.-C. Bordage, *Contribution à l'étude de la cinétique électronique dans un gaz faiblement ionisé*. PhD thesis, Université Paul Sabatier de Toulouse, 1995.

[29] S. Yoshida, A. V. Phelps, and L. C. Pitchford, "Effect of electrons produced by ionization on calculated electron-energy distributions," *Physical Review A*, vol. 27, no. 6, 1983.

[30] N. R. Pinhão and M. Vranic, "Electron transport parameters and rate coefficients in $He/CH_4/O_2$ and $He/CH_4/CO_2$ mixtures," in *XX ESCAMPIG*, no. July, 2010.

[31] T. Shirai, T. Tabata, H. Tawara, and Y. Itikawa, "Analytic Cross Sections for Electron Collisions With Hydrocarbons: CH_4, C_2H_6, C_2H_4, C_2H_2, C_3H_8, and C_3H_6," *Atomic Data and Nuclear Data Tables*, vol. 80, no. 2, pp. 147–204, 2002.

[32] P. Rawat, V. S. Prabhudesai, M. Rahman, N. B. Ram, and E. Krishnakumar, "Absolute cross sections for dissociative electron attachment to NH_3 and CH_4," *International Journal of Mass Spectrometry*, vol. 277, no. 1-3, pp. 96–102, 2008.

[33] D. K. Davies, L. E. Kline, and W. E. Bies, "Measurements of swarm parameters and derived electron collision cross sections in methane," *Journal of Applied Physics*, vol. 65, no. 9, p. 3311, 1989.

[34] "IST-Lisbon database." www.lxcat.net, Jan. 2012.

[35] "LAPLACE database." www.lxcat.net, Dec. 2011.

[36] J. de Urquijo, I. Alvarez, E. Basurto, and C. Cisneros, "Measurement of ionization and electron transport in methane-argon mixtures," *Journal of Physics D: Applied Physics*, vol. 32, no. 14, p. 1646, 1999.

[37] S. R. Hunter, J. G. Carter, and L. G. Christophorou, "Electron transport measurements in methane using an improved pulsed Townsend technique," *Journal of Applied Physics*, vol. 60, no. 1, p. 24, 1986.

[38] L. M. Chanin and G. D. Rork, "Experimental Determinations of the First Townsend Ionization Coefficient in Helium," *Phys. Rev.*, vol. 133, p. A1005, 1964.

[39] D. K. Davies, F. Llewellyn-Jones, and C. G. Morgan, "Primary ionisation coefficient in helium," *Proc. Phys. Soc.*, vol. 80, p. 898, 1962.

[40] C. S. Lakshminarasimha and J. Lucas, "The ratio of radial diffusion coefficient to mobility for electrons in helium, argon, air, methane and nitric oxide," *Journal of Physics D: Applied Physics*, vol. 10, p. 313, 1977.

[41] T. Belmonte, R. P. Cardoso, G. Henrion, and F. Kosior, "Collisional–radiative modelling of a helium microwave plasma in a resonant cavity," *Journal of Physics D: Applied Physics*, vol. 40, pp. 7343–7356, 2007.

[42] Y. Nakamura, "Drift Velocity and Longitudinal Diffusion Coefficient of Electrons in CO_2-Ar Mixtures and Electron Collision Cross Sections for CO_2 Molecules," *Aust. J. Phys.*, vol. 48, no. July 1994, pp. 357–364, 1995.

[43] "NIFS Database (National Institute for Fusion Science)." http://dpc.nifs.ac.jp/DB/IEEJ/.

[44] M. Hayashi, "Electron collision cross sections determined from beam and swarm data by Boltzmann analysis," in *Nonequilibrium Processes in Partially Ionized Gases* (M. Capitelli and J. Bardsley, eds.), Plenun Press, 1990.

[45] S. Buckman, M. Elford, and D. Newman, "Electron scattering from vibrationally excited CO_2," *Journal of Physics B: Atomic and Molecular Physics*, vol. 20, p. 5175, 1987.

[46] M. T. Elford, "The Drift Velocity of Electrons in CO_2 at 293^oK," *Austr. J. Phys.*, vol. 19, p. 629, 1966.

[47] Y. Itikawa, "Cross Sections for Electron Collisions With Carbon Dioxide," *Journal of Physical and Chemical Reference Data*, vol. 31, p. 749, Sept. 2002.

[48] S. Buckman and A. Phelps, "Tabulations of collision cross sections and calculated transport and reaction coefficients for electrons in H_2 and D_2," Tech. Rep. 27, JILA, 1985.

[49] J. E. Land, "Electron scattering cross sections for momentum transfer and inelastic excitation in carbon monoxide," *Journal of Applied Physics*, vol. 48, p. 5716, 1978.

[50] "Phelps database." www.lxcat.net, Sept. 2012.

[51] A. Janeco, N. Pinhão, and V. Guerra, "Electron kinetics in mixtures of CH_4, CO_2 and He, with formation of H_2 and CO: the effects of composition and vibrational temperature ," in *XXXI ICPIG*, 2013.

[52] S. K. Dhali and P. F. Williams, "Numerical simulation of streamer propagation in nitrogen at atmospheric pressure," *Physical Review A*, vol. 31, no. 2, pp. 1219–1222, 1985.

[53] U. Kogelschatz, "Dielectric-barrier Discharges: Their History, Discharge Physics, and Industrial Applications," *Plasma Chemistry and Plasma Processing*, vol. 23, no. 1, pp. 1–46, 2003.

[54] R. Snoeckx, M. Setareh, R. Aerts, P. Simon, A. Maghari, and A. Bogaerts, "Influence of N_2 concentration in a CH_4/N_2 dielectric barrier discharge used for CH_4 conversion into H_2," *International Journal of Hydrogen Energy*, vol. 38, pp. 16098–16120, Dec. 2013.

[55] V. Goujard, J.-M. Tatibouët, and C. Batiot-Dupeyrat, "Carbon Dioxide Reforming of Methane Using a Dielectric Barrier Discharge Reactor: Effect of Helium Dilution and Kinetic Model," *Plasma Chemistry and Plasma Processing*, vol. 31, pp. 315–325, Jan. 2011.

[56] A. Fridman, *Plasma Chemistry*. Cambridge University Press, 2008.

[57] A. Jelenak, J. V. Jovanović, S. A. Bzenić, S. S. Vrhovac, B. Tomčik, and Z. Lj. Petrović, "The influence of excited states on the kinetics of excitation and dissociation in gas mixtures containing methane," *Diamond and Related Materials*, vol. 4, pp. 1103–1112, 1995.